MAP Stability, Design and Analysis

A. J. Ericsson-Jackson, S. F. Andrews, J. R. O'Donnell, Jr., F. L. Markley
NASA Goddard Space Flight Center, Code 570, Greenbelt, MD, 20771

Abstract

The Microwave Anisotropy Probe (MAP) is a follow-on to the Differential Microwave Radiometer (DMR) instrument on the Cosmic Background Explorer (COBE) spacecraft. The design and analysis of the MAP attitude control system (ACS) have been refined since work previously reported. The full spacecraft and instrument flexible model was developed in NASTRAN, and the resulting flexible modes were plotted and reduced with the Modal Significance Analysis Package (MSAP). The reduced-order model was used to perform the linear stability analysis for each control mode, the results of which are presented in this paper. Although MAP is going to a relatively disturbance-free Lissajous orbit around the Earth-Sun L_2 Lagrange point, a detailed disturbance-torque analysis is required because there are only a small number of opportunities for momentum unloading each year. Environmental torques, including solar pressure at L_2, aerodynamic and gravity gradient during phasing-loop orbits, were calculated and simulated. Thruster plume impingement torques that could affect the performance of the thruster modes were estimated and simulated, and a simple model of fuel slosh was derived to model its effect on the motion of the spacecraft. In addition, a thruster mode linear impulse controller was developed to meet the accuracy requirements of the phasing loop burns. A dynamic attitude error limiter was added to improve the performance of the ACS during large attitude slews. The result of this analysis is a stable ACS subsystem that meets all of the mission's requirements.

INTRODUCTION

The Microwave Anisotropy Probe (MAP), one of the first two Medium-Class Explorer (MIDEX) missions, will measure the anisotropy of the Cosmic Microwave Background (CMB), which is believed to be a remnant of the Big Bang, or Primordial Fireball, marking the birth of the universe.[1] This anisotropy was first measured by the Differential Microwave Radiometer (DMR) instrument on the Cosmic Background Explorer (COBE) satellite.[2-4] MAP has been designed to measure the spectrum and spatial distribution of the CMB with sensitivity 50 times that of the DMR and angular resolution 20 times finer, specifically 0.3° or 18 arc-minutes. These increases in sensitivity and resolution should enable MAP to determine the values of key cosmological parameters and to answer questions about the formation of structure in the early universe.

MAP is scheduled to launch in the Fall of 2000 on a Delta launch vehicle, and will be placed in a Lissajous orbit around the Sun-Earth L_2 point using a lunar assist with phasing loops,

reaching its final orbit approximately 100 days after launch. The MAP radiometers cover two fields of view (FOVs) 135° apart on the celestial sphere. To obtain a highly interconnected set of measurements over a large area of the celestial sphere, the MAP observatory will execute a fast spin (0.464 rpm) and a slower precession (0.1°/sec) of its spin axis about the Sun line. The entire celestial sphere will be observed once every six months, or four times in the planned on-station mission life of two years.

There are six ACS operational modes: Inertial, Observing, Delta V, Delta H, Sun Acquisition, and Safehold. Inertial mode acts as a staging mode between the other operations of the spacecraft; it can either hold the spacecraft in an inertially-fixed orientation or slew the spacecraft between two different orientations. Observing mode is used for science operations. Delta V mode uses the thrusters (REM) to adjust the orbit. Delta H mode uses the REMs to unload excess angular momentum. Sun Acquisition mode acquires and maintains a thermally-safe power-positive orientation of the spacecraft. Safehold mode puts the spacecraft in a power- and thermal- safe attitude.

The remainder of the paper will present various analyses of the MAP ACS. The effect of flexible modes, reaction wheel jitter, and fuel slosh on pointing stability a performance will be discussed. Estimates of thruster plume impingement torques and environmental torques in the phasing loops, lunar swingby, and final L_2 orbit will be presented, along with contingency procedures for managing these torques. A linear impulse controller designed to improve the accuracy of MAP's thruster firings will also be discussed. Lastly, a dynamic attitude error limiter was added to improve the performance of the ACS during large attitude slews; this will be presented as well.

STRUCTURAL MODEL

Reduced Order Flexible Modes

Initially, NASTRAN[5] modeled large bodies like the antenna and thermal reflector as point masses. The newer NASTRAN model incorporated the physical dimensions of these large appendages and instruments. With these new inclusions the dominant flexible mode frequencies increased from 1.9 Hz to 5.7 Hz. From this model a reduced order flexible model has been created which reduced the system to include only 3-4 dominant modes for each Spacecraft Mode. By using the MSAP[6] software, the associated energy for each mode was compared through the formulation of various summary methods: Frequency, Modal Gain, Peak Amplitude and Gregory's Method which are listed below in Table 1. In addition, each mode's singular value plots for the rigid body, the flexible modes, and a combination of the two were analyzed. The current estimated dominant mode frequencies are 5.744, 5.787, 27.73, 33.26, 36.2 and 44.93 Hz.

The structural system is fairly rigid; therefore, the flexible modes have less effect on the spacecraft system's stability. As a result, the majority of analysis were done for a plant derived as a combination of the rigid body modes and the chosen dominant flexible modes. The various structural plants analyzed were: 1) the rigid body modes, 2) the rigid body modes plus flexible body modes, and; 3) the rigid body plus the reduced flexible body modes (respectively, line 1, 2 and 3 in Figure 1). The system plant was modeled as the Plant = $1/(Is^2)$ + Flexible modes, where, I is the spacecraft inertia. Since the inertia values change by less than 1% (0.1 dB) from "Beginning of Life" to "End of Life" stability analysis will hold for all phases of the mission.

Table 1
DOMINANT FLEXIBLE MODES

Modes	Freq. Hz	Modal Gain	Peak Ampl.	Gregory	Actuators	Sensors
Inertial/Observing						
11	5.744	6.537	98.33	100	Rotation Theta_x,y,z	Rotation Theta_x,y,z
12	5.787	6.749	100	100	Wheels1,2,3	IRU
27	33.26	20.85	9.35	11.38		
34	44.93	100	24.58	20.08		
Delta V/H						
7	5.272	14.48	100	100	Translation	Rotation Theta_x,y,z
11	5.744	37.95	45.29	46.62	Thrusters	IRU
27	33.26	41.59	3.27	2.764	1,2,3,4,5,6,7,8	
40	46.16	100	4.08	7.5		
Safehold						
11	5.744	14.75	97.49	100	Rotation Theta_x,y,z	Rotation Theta_x,y,z
22	27.73	50.29	14.26	8.35	Wheels1,2,3	CSS 1,3,5
34	36.82	100	16.08	15.12		
Sun Acquistion						
11	5.744	14.75	97.49	100	Rotation Theta_x,y,z	Rotation Theta_x,y,z
(not used in analysis)12	5.787	15.36	100	91.31	Wheels1,2,3	CSS 1,3,5
22	27.73	50.29	14.26	8.34		IRU
34	36.82	100	16.08	15.101		

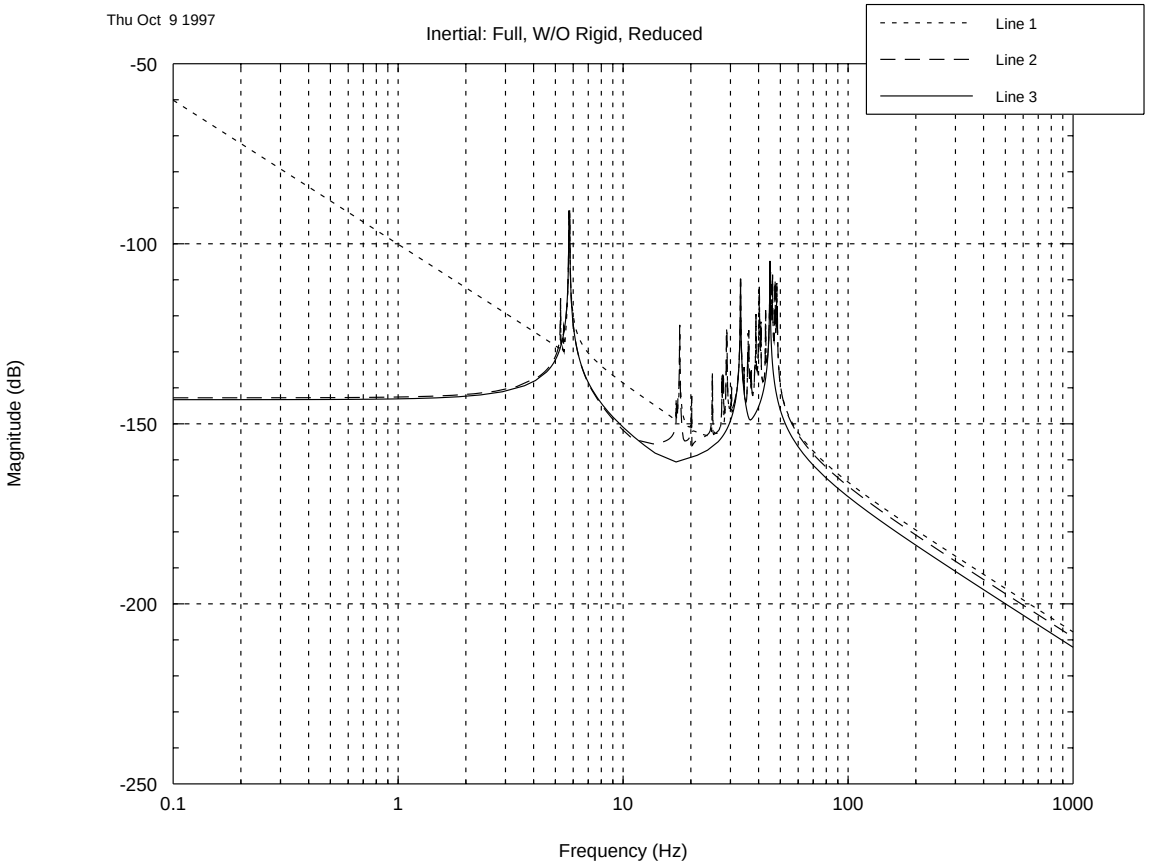

Figure 1. Singular Value Plot of Flexible modes for MAP

Stability

Nichols stability charts were created for each spacecraft system mode in INCA[7,8]. The dynamic plant prescribed as a structural plant multiplied by the gyro dynamics (a simple second order system) was included in a closed loop feedback system with a proportional derivative (PD) controller. By implementing the Nichols and Bode techniques, the proportional and rate controller gains were used to calculate the stability margins for all the modes. All of the modes except one satisfied the Guidance Navigation and Control Center design criteria of at least 12 dB phase margin and 30° gain margin. Typically, the gain margin fell between 14-22 dB and the phase margin was between 36°-81°. Since the Safehold Mode Y-axis was unable to meet the required bounds, it was necessary to add a low pass structural filter in that axis. The addition of a structural filter to the dynamic plant produced the Nichols plot shown in Figure 2.

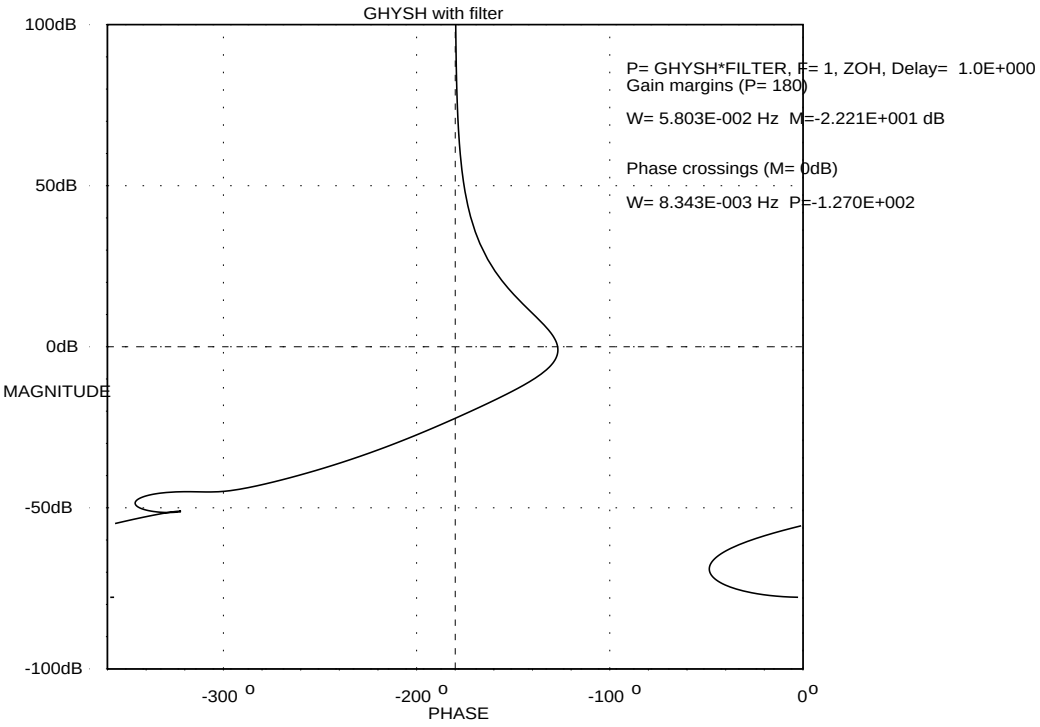

Figure 2. Nichols Stability Chart for Safehold Mode Y-axis

WHEEL JITTER RESONANCE

Since Observing mode requirements are so stringent it was necessary to examine wheel jitter resonance. This wheel jitter resonance is due to the dominant flexible modes resonating with the wheel imbalance torques. The forces and torques due to structural resonance are described as:

$$\begin{aligned} F_x &= \Delta_{sr} * \omega_r^2; T_x = \Delta_{sr} * \omega_r^2 * L_{zr} + \Delta_{dr} * \omega_r^2 \\ F_y &= \Delta_{sr} * \omega_r^2; T_y = \Delta_{sr} * \omega_r^2 * L_{zr} + \Delta_{dr} * \omega_r^2 \\ F_z &= 0.0; T_z = \Delta_{sr} * \omega_r^2 * \sqrt{L_{xr}^2 + L_{yr}^2} \end{aligned} \quad (1)$$

where, ω_r is the wheel's angular velocity, L is the length to the wheel from the gyroscope, and Δ_{sr} and Δ_{dr} are the static and dynamic imbalance of the wheels, respectively.

MAP's wheels have associated imbalance values of Δ_{sr} =2.5E-5 kg-m and Δ_{dr}=2.5E-5 kg-m^2. Two angular velocities were considered: the first wheel frequency was near the flexible mode of 44.94 Hz and the second one is when the 3 wheels are running simultaneously at 25 Hz, near the (28.95 Hz flexible mode. The body rotation torques seen at the gyroscope due to wheel resonance were calculated to be between 22.7–36.1 arc-sec at 44.94 Hz and between 1.04-1.65 arc-sec at 25 Hz. This analysis showed that the wheel jitter in resonance with the flexible mode frequencies does not cause problems with MAP's Observing Mode pointing requirements.

ENVIRONMENTAL TORQUES

The environmental disturbance torques that may act upon the spacecraft while it is orbiting the Earth are as follows: aerodynamic, gravity gradient, solar radiation and magnetic.[9] Since most of MAP's orbit is very high, torques due to the Earth's magnetic field are not significant.

Orbit Phasing Loops

After MAP's injection into orbit about the Earth there are multiple phasing loops. During these loops the thrusters will burn to increase the eccentricity and semimajor axis of the orbit, placing the vehicle in position for a lunar swingby. In this orbit, drag is the most important external torque at perigee because the density of the planet's atmosphere increases exponentially as the altitude decreases. Therefore, at the perigee altitude, a maximum aerodynamic force and torque were calculated. In addition, the gravity gradient torque and resultant momentum buildup are computed for both the Earth and the Moon.

Aerodynamic Torques. The drag torque and momentum build up is calculated for the portion of the Earth's orbit below 1000 km altitude. Initially, the sun-side surface areas are utilized to calculate the aerodynamic forces. These areas are primarily made up of the Solar panels, the Teflon webbing, and the middle spacecraft body hexagon. A three-dimensional model of MAP was created in SPAD[10]. All momentum values were calculated by multiplying the torque by the total elapsed time of 1 day. At the perigee altitude, the maximum aerodynamic force and torque are 0.0471 N and 7.68×10^{-4} N-m respectively. The orbital altitude is less than from 1000 km for approximately 7 minutes, which produces a momentum of 0.32 N-m-s. The sun-side SPAD results that were averaged during one rotation verified that the average torque is only 3.367×10^{-4} N-m and the momentum is 0.14 N-m-s. The density, velocity and aerodynamic torque were plotted as a function of altitude. The SPAD results for the x and y face exposure were put into SystemBuild[11] and simulated during the portion of the orbit when the altitude was 2250 km to 300 km to 2250 km. The simulation produced data very similar to the previous SPAD results. The maximum x and y face aerodynamic torque is 0.012 N-m and the momentum has a peak of 0.47 N-m-s and an average of 0.28 N-m-s.

Gravity Gradient for Earth. The calculation of the Earth gravity gradient torque on the spacecraft and the momentum buildup are calculated and simulated for the portion of the Earth orbit below the altitude of 1000 km. The Earth's gravity gradient momentum and an average

torque were calculated to be 0.1744 N-m-s and 2.0×10^{-4} N-m in the x-direction, and 0.221 N-m-s and 4.1×10^{-5} N-m in the z-direction. Gravity gradient simulation results further verified values for torque and momentum buildup. The Earth gravity gradient simulations displayed a maximum torque of 1.7×10^{-4} N-m in the x and y-axes and 1.0×10^{-5} N-m in the z-axis and a maximum momentum of 0.15 N-m-s in the x and y axes, 0.07 N-m-s in the z-axis, and a maximum system momentum of 0.15 N-m-s.

Lunar Swingby

As previously mentioned the phasing orbits insert the spacecraft into the proper trajectory for a lunar swingby. As a result, the gravity gradient torque and momentum associated with the Moon's environment were calculated. These values were computed for a 20 minute portion of the orbit during the closest approach to the Moon, which is approximately 1000 km.

Gravity Gradient for Moon. The torque and momentum values for the Lunar gravity gradient torque on the spacecraft are 0.0736 N-m-s and 3.6×10^{-5} N-m in the x-direction, and 0.064 N-m-s and 5.0×10^{-6} N-m in the z-direction. Gravity gradient simulation results further verified values for torque and momentum buildup. Lunar gravity gradient simulations displayed a maximum torque of 3.5×10^{-5} N-m in the x and y axes and 2.5×10^{-6} N-m in the z-axis and a maximum momentum of 0.04 N-m-s in the x and y axes, 0.026 N-m-s in the z-axis, and a maximum system momentum of 0.047 N-m-s.

Libration Point

After MAP's lunar swingby, the spacecraft will be in orbit about the Earth-Sun L_2 point. The solar radiation pressure and a solar pinwheel torque associated with a solar array deployment misalignment have been calculated. For these computations, the primary surface areas exposed to the Sun are the solar array panels, the silver Teflon webbing, and a black and white painted hexagon. For the solar pinwheel torque, the hexagon area in the middle of the z-face was excluded because it will not experience an angular deflection due to deployment.

Solar Radiation Pressure. The calculated values of solar radiation result in an instantaneous Solar pressure torque (T_{solar}) and average momentum buildup (ΔH_{solar}) of 1.85×10^{-6} N-m and 0.16 N-m-s per day. Under ideal conditions the T_{solar} and ΔH_{solar} about spin and precession axes average out to zero. With a misalignment tolerance of $\pm0.25°$ about the spin axes the T_{solar}= 1.07×10^{-8} N-m and ΔH_{solar}= 9.3×10^{-4} N-m-s for a period of 1 day. For further verification these calculated values were compared to SPAD generated data. Results from SPAD produced an average solar torque and momentum buildup per day of 1.88×10^{-8} N-m and 0.00162 N-m-s. It was realized that calculations could be off by an order of magnitude because of different assumptions and the greater precision of the SPAD method.

Pinwheel Torque. The solar arrays may deploy improperly resulting in a canted surface area. A combination of their tilted surface and the solar pressure torque could cause a pinwheel torque, which is a torque about the spacecraft spin (z) axis This disturbance effect has been calculated for a solar array canted angle of 1° and a spin axis misalignment of ±0.5°.

The maximum instantaneous pinwheel torque and the accumulated momentum in the z-axis are 1.46×10^{-6} N-m and 0.126 N-m-s/°-day. The average momentum buildup per day in the x and y-axes (with a misalignment angle of 0.5° in the spin axis) are 0.0736 N-m-s and 0.0645 N-m-s, respectively. The SPAD pinwheel torque and momentum results have been produced for

two cases. For the maximum case of the sun vector parallel to the normal vector they are 5.82×10^{-7} N-m and 0.0503 N-m-s, respectively. For a pitch sunline angle of 22.5° the torque and momentum are 5.31×10^{-7} N-m and 0.0459 N-m-s, respectively.

The SPAD data were curve-fit to produce the torque and momentum equations. After integrating the torque to get the momentum and using zero initial conditions for the momentum; a maximum system momentum magnitude of 1 Nms leads to a buildup time of 23.36 days. However, it was found that the SPAD model has errors due to:

1) Solar array and webbing areas are too small by 35%; these areas are 2/3 of the total bottom area. This leads to an error of 23%, and

2) The moment arms are off by 11.7% due to smaller solar array length than originally thought.

The total system momentum buildup for one day becomes 0.059 N-m-s and the total time for the momentum to buildup to 1.5 N-m-s is 25.5 days. The data presented could mean that a momentum dump has to be performed every 3-4 weeks. For each simulation that will run later the momentum vector in the body frame will be initialized to $[0, \pm1.5, \pm1.5]/\sqrt{2}$. The system's momentum tolerance is 1.5 N-m-s and the total time between unloading burns is 90 days; the maximum solar array deployment misalignment angle is 0.228°. See Table 2 for summary of environmental torques and momentum.

Table 2
Summary of Environmental Disturbances

Calculated Disturbances	**Torque (N-m)**	**Momentum (N-m-s)**
Aerodynamic Phasing Burn	7.68E-4 (@300km)	0.32 @ t =7min (1000 km)
Gravity Gradient Phasing Burn	Tx=2E-4, Tz=4.1E-5	Hx=.174, Hz=0.221 @1 orbit
Gravity Gradient Lunar Swingby	Tx=3.6E-5, Tz=5E-6	Hx=.073, Hz=0.064 @1 orbit
Solar Pressure (instantaneous)	Tx=1.85E-6	Hx=0.16 @ t=1 day
Solar Pressure (average)	Tx=1.07E-8	Hx=9.3E-4 @ t=1 day
Solar Pinwheel (instantaneous)	Tx,y,z=1.23E-4,1.32E-4,1.46E-6	Hx=10.6,Hy=10.06,Hz=.126 @1day
Solar Pinwheel (average)		Hx=0.073 & Hy=0.064 @1day

Simulated Disturbances	**Torque (N-m)**	**Momentum (N-m-s)**
Aerodynamic Phasing Burn SPAD z-face	3.147E-4 (@300km)	0.131 @ t =7min (1000 km)
Aerodynamic Phasing Burn SPAD x&y-face	0.012 (2250km=>300km=>2250km)	0.47 (peak), 0.28 (avg)
Gravity Gradient Phasing Burn SB	Tx=1.7E-4, Tz=1.0E-5	Hx=0.15, Hz=0.07 @1 orbit
Gravity Gradient Lunar Swingby SB	Tx=3.5E-5, Tz=2.5E-6	Hx=0.04, Hz=0.026 @1 orbit
Solar Pressure (average) SPAD	Tx=1.88E-8	Hx=1.62E-3 @ t=1 day
Solar Pinwheel (average) SPAD	Tx=5.31E-7	Hx=0.0459 @ t=1 day
SPAD- Solar Pressure & Aerodynamic Drag		SB- System Build

Solution for Handling Environmental Torques

As a response to the concern about the pinwheel torque, a method was developed to unload excess system momentum while in Observing Mode, using a series of three "one shot" thruster firings. This algorithm is not currently baselined to be flown on MAP, but was developed as a contingency procedure in the event that system momentum build-up on station is greater than expected. The algorithm was designed to meet the following constraints and design goals:

1. Unload momentum to less than 0.3 Nms while in Observing Mode.

2. Always keep the solar arrays normal within 25° of the sunline (violations of the 22.5±0.25° Observing Mode sunline angle constraint are permissible).
3. Perform the entire operation during one ground pass (37 minutes)

Using the MAP thruster pair 1 and 2 as an example, the steps in this process are as follows,:

A. Wait until the momentum transverse to the z-axis is all in the +x axis. Fire thruster 2 to remove as much of this momentum as possible.
B. After thruster firing A, wait until the sun is in the (–x,z) quadrant of the x-z plane. Fire thruster 1 or 2 (depending on the sign of the z-axis momentum) to add x momentum equal to the amount of momentum in the z-axis. By doing this, the system momentum vector is positioned such that half a precession cycle later it will be almost entirely in the +x-axis. This results in an intermediate system momentum state as much as $\sqrt{2}$ higher than the initial value, but simulations show that this system momentum value does not pose an attitude control problem.
C. After thruster firing B, wait approximately half of a precession cycle (30 minutes), and then wait until all of the system momentum is in the +x axis. Fire thruster 2 to remove as much of this momentum as possible.

The total procedure requires a maximum of 35.5 minutes and reduces system momentum is to near zero. The algorithm could be adjusted to use only one of the two thrusters, or to use one of the other two thruster sets.

THRUSTER PLUME IMPINGEMENT TORQUES

Fuel Slosh

Propellant slosh is a mechanical effect of liquid propellants. At the moment the propellant mass impacts the wall of the fuel tank, it will transfer momentum to the spacecraft. If the tank is not at the center of mass of the vehicle, this will create an impulse moment that will affect the vehicle attitude. This disturbance can be significant and unacceptable, and must be limited through tank design. Fortunately, the MAP tank is close to the center of mass and the moment arm is small. In addition, a flexible membrane (diaphragm) has been placed in the tank to assure that the propellant remains in contact with the propellant port and to help damp out the sloshing effects.

The original analysis for the ACS Critical Design Review used a model for fuel slosh that was found in two reports.[12, 13] The TDRS slosh model from NASA CR 166745 report[12] is presented in Figure 3. According to that model, the slosh natural frequency, ω_n depends on the torsional spring constant, K, and the overall acceleration, a, of the tank:

$$\omega_n = \sqrt{\frac{K}{M_1 L^2} + \frac{a}{L}}\,. \tag{2}$$

Figure 4 is the model used in a study for the CRAF/Cassini spherical tanks.

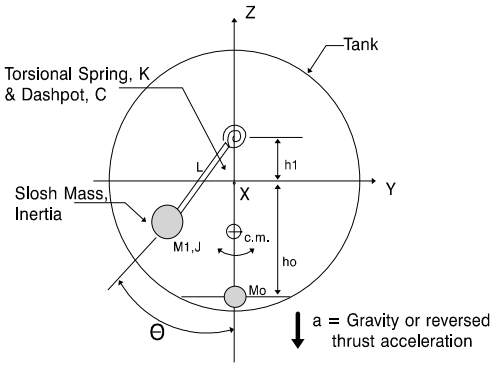

Figure 3. TDRS Fuel Slosh Model

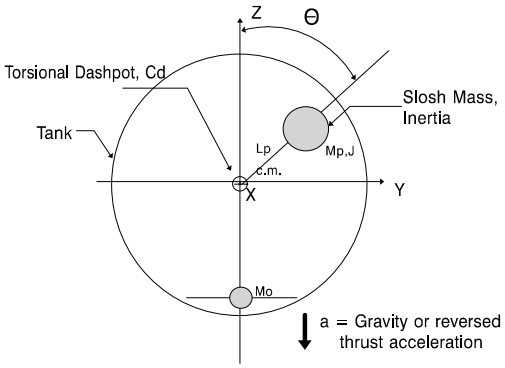

Figure 4. Cassini Fuel Slosh Model

The angular position, θ, of the model pendulum is a representation of the position of the liquid bulk and the lateral offset, Z_{cg}, of the liquid center with respect to the direction of the settling acceleration can be calculated as (see Figure 4):

$$z_{cg} = \frac{M_p L_p \cos\theta}{M_p + M_o}. \tag{3}$$

Assume $\theta = \frac{\pi}{4}\sin\omega_n t$, where the natural frequency of the slosh material is defined as in the TDRS report already presented. Then the equations of motion for the system are defined as:

linear torque, $T_{linear} = r \times F = r_{cm} \times M\omega^2 r = r_{cm} L M_1 \frac{\pi^2 \omega_n^2}{16}\cos^2\omega_n t$, (4)

angular torque, $T_{angular} = J\ddot{\theta} = -J\frac{\pi\omega_n^2}{4}\sin\omega_n t$, and (5)

angular momentum, $H_{angular} = J\dot{\theta} = -J\frac{\pi\omega_n}{4}\cos\omega_n t$. (6)

From the initial analysis, the calculated fuel slosh inertia, J is 0.007 % of the total system inertia and the derived natural frequency, ω_n is several times larger than the system's bandwidth frequency, 0.02 Hz.

The previous reports had several questionable aspects. However, one of the models did not include a stiffness factor and the equation for the natural frequency was incorrect for the corresponding dynamic equation. Therefore, it was necessary to derive our own scenario for each aspect of the fuel slosh's movement. The five worst cases considered were:

(1) Radial Thrust with a full tank of fuel;
(2) Slew Maneuver with a full tank and a half full tank;
(3) Linear Station Keeping Effects at L_2 (half tank);
(4) Angular Station Keeping Effects at L_2 (half tank); and
(5) Observing Mode Fast Spin, accelerating and constant rate (all ranges of fuel).

Simple models were drawn for each case to obtain dynamic equations describing the motion of the fluid. Further research was done to find a better value for the stiffness coefficient, K and the damping coefficient, C. Values for K and C could be associated with MAP's diaphragm thickness (0.12 in) and were extrapolated from References 14-15. The results are shown below in Figure 5. Calculation of the torques and momentum buildup due to the fuel slosh were done for

each case. In addition, an angular response due to the fuel slosh torque was calculated, $\frac{\theta}{T_{fs}} = \frac{1}{Is^2}$. The basic block diagram for the analytical system is shown in Figure 6.

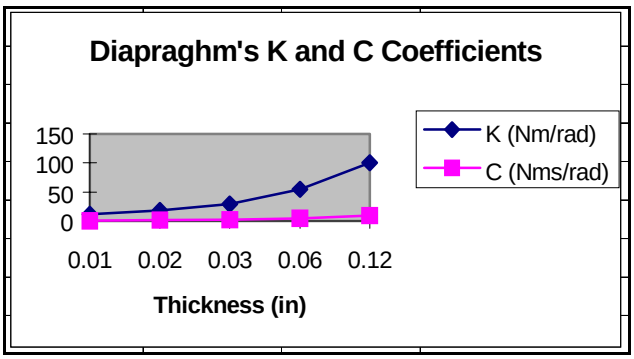

Figure 5. Extrapolation of MAP's K and C with Diaphragm Thickness

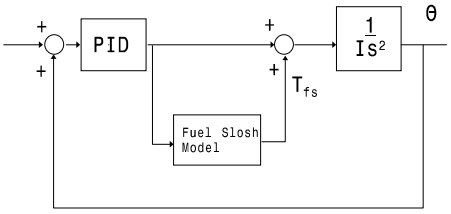

Figure 6. Block Diagram to Analyze Angular Effect due to Fuel Slosh

All the results for the various cases are presented below.

Case 1- Radial Thrust with a full tank of fuel:
The angular frequency was 1.05 to 1.5 Hz, the linear torque was 3.65×10^{-5} to 7.52×10^{-5} N-m, the angular torque was 0.055 to 0.025 N-m, and the angular momentum was 0.004 to 0.001 N-m-s.

Case 2- Slew Maneuver with both a full and half full tank a fuel:
The angular frequency was 1.04 to 1.5 Hz, the linear torque ranged from 0.752-0.69 N-m, the angular torque ranged from 4.13-6.36 N-m and the angular momentum ranged from 0.55-1.24 N-m-s.

Case 3- Linear Station Keeping Effects at L_2 (half a tank):
Radial Thrusting produces an angular frequency of 1.64 to 2.05 Hz, a linear torque of 8.54×10^{-5} to 1.13×10^{-4} N-m, an angular torque of 0.011 to 0.02 N-m and an angular momentum ranging from 0.0007 to 0.001 N-m-s.
Perpendicular Thrusting produces an angular frequency of 6.23 to 8.25 Hz, a linear torque of 11 N-m, an angular torque of 61 N-m and an angular momentum ranging from 1.5 to 2 N-m-s.

Case 4- Angular Station Keeping Effects at L_2 (half a tank):
The angular frequency was 1.62 to 2.04 Hz, the linear torque was 0.69 N-m, the angular torque was between 3.76-4.19 N-m and the angular momentum ranged from 0.37-0.52 N-m-s.

Case 5- Observing Mode Fast Spin, accelerating and constant rate (for all ranges of fuel).
A constant angular rate applied to the spacecraft produced an angular frequency of 0.39 to 0.503 Hz, a linear torque between 4.6×10^{-6}-1.3×10^{-5} N-m, the angular torque was between 0.0014-0.002 N-m and the angular momentum ranged from 1.33×10^{-5}-1.7×10^{-5} N-m-s.
An angular acceleration applied to the spacecraft produced an angular frequency of 0.39 to 0.503 Hz, a linear torque between 0.01-0.017 N-m, the angular torque was between 0.00013-0.00017 N-m and the angular momentum ranged from 6.4×10^{-5}-8.9×10^{-5}N-m-s.

After this analysis, it was found that fuel slosh would not have a large affect on the spacecraft's attitude. Although some of the instantaneous torque and momentum values are large, their overall effect was small. The natural frequency of the slosh system is several orders of magnitude larger than the bandwidth of the control system. The angular displacement due to either the linear or angular torque is from 10^{-9} to 10^{-5} radians. This analysis determined that fuel slosh should not be a concern to the MAP mission.

CONTROLLERS

Thruster Mode Linear Impulse Controller

The Thruster Mode linear impulse controller was designed to improve the accuracy of MAP's z-axis Delta V's. There are some tradeoffs involved in usage of this impulse controller; with the impulse controller the spacecraft uses about 12% more fuel, without it, errors during Delta V are about 12% larger. Current implementation allows for burn accuracy of less than 1 sec but this could be improved to 0.04 sec if necessary. This excludes subsequent firings in the Delta H mode.

The operational plan is to enable the impulse controller right after MAP's lunar swingby during the mid-course correction (MCC) so it is available L_2. At L_2, the absolute duration of the burns is smaller so the percentage errors tend to be higher. Without the impulse controller the burn is corrected with a one-sided impulse controller in both x and z. Regardless of whether or not the impulse controller is enabled, the current design will ensure that the burn duration will be at least the desired amount of time. Figures 7 and 8 shows a sample L_2 burn with and without the impulse controller, respectively; the commanded thruster time for each run was 60 seconds in the x-axis and 30 seconds in the z-axis. Notice the error caused without the impulse controller and the extra thruster firings to correct the error with it.

Dynamic Attitude Error Limiter

The dynamic rate limiter enables the spacecraft to meet the sunline requirement during a slew in Inertial Mode. When the limiter is not utilized, Inertial Mode slews that include high spin errors in the z-axis can cause the spacecraft to violate the 25° sun constraint, as shown in Figure 9. The dynamic rate limiter calculates an attitude error limit for each axis proportional to the error in that axis. This preserves the direction of the resulting Inertial Mode slew and prevents the spacecraft from violating the sun constraint as in Figure 10. Both Figures 9 and 10 show a series of 45° Inertial Mode slews across the sunline with spin angles from 0° to 180°; with the dynamic attitude error limiter, the spacecraft on these slews does not violate the sun constraint.

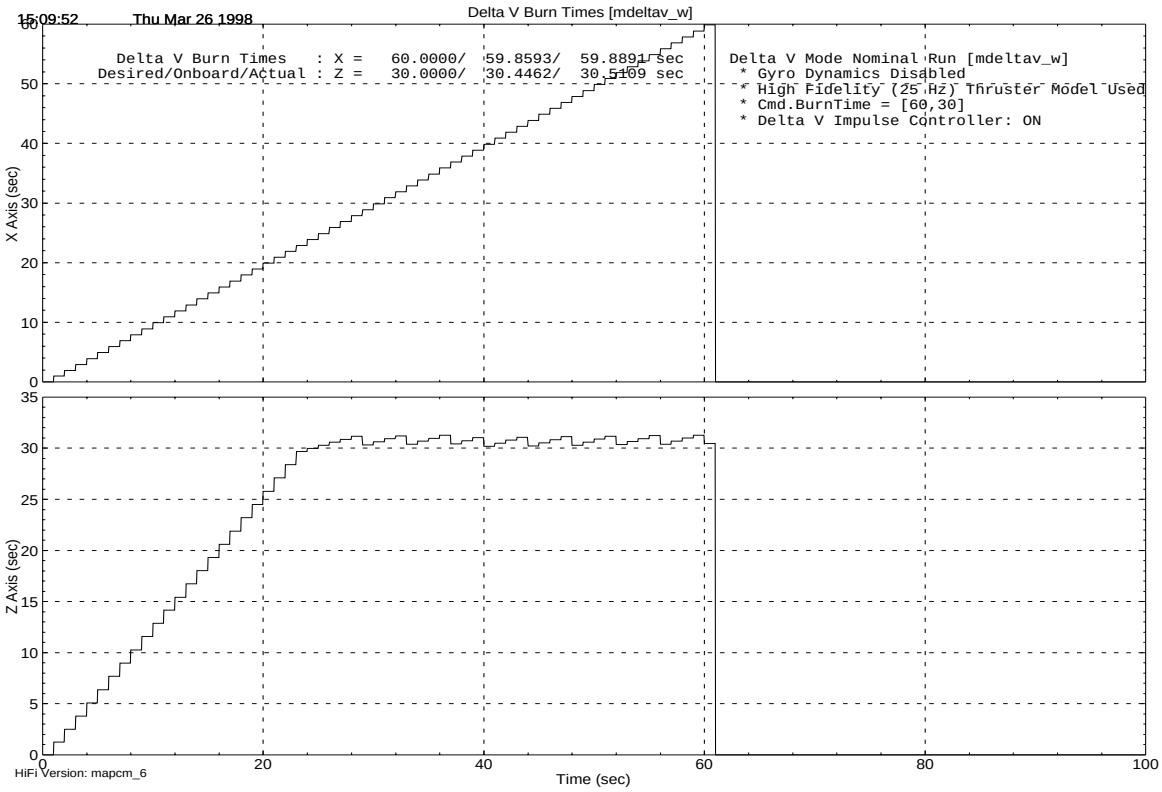

Figure 7. Delta V burntime in X & Z axis with impulse controller

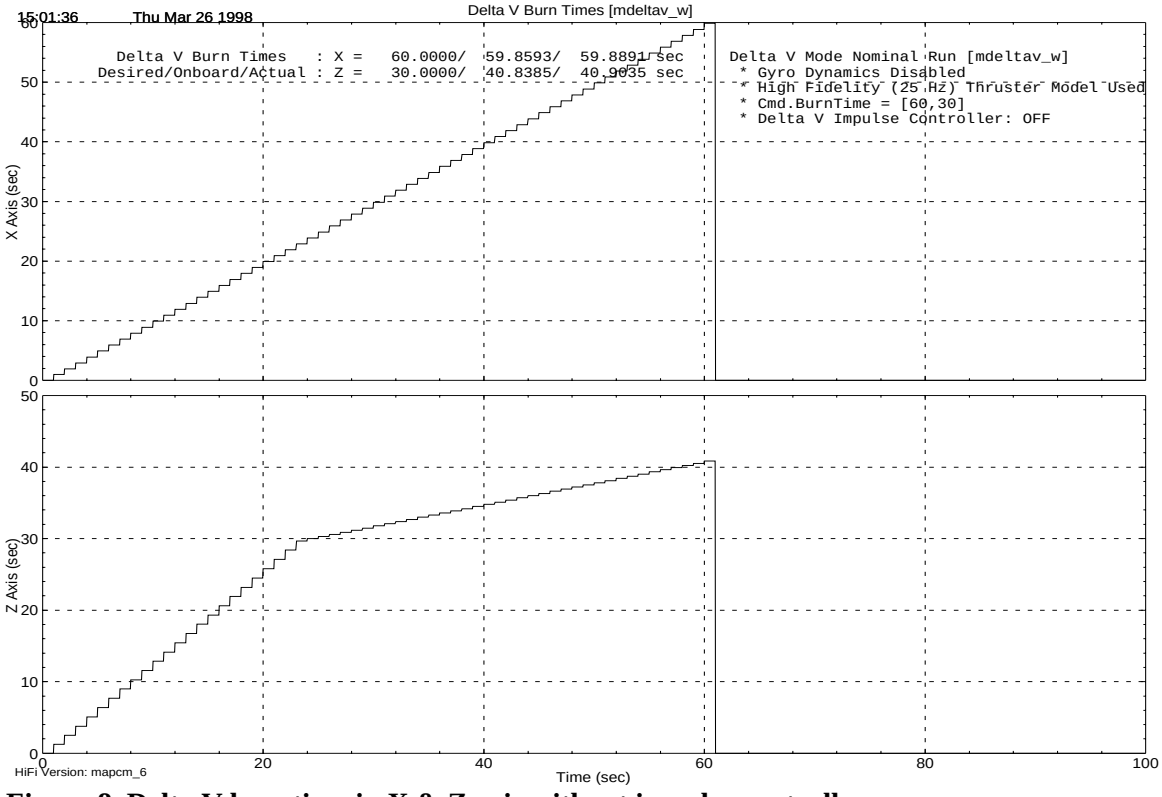

Figure 8. Delta V burntime in X & Z axis without impulse controller

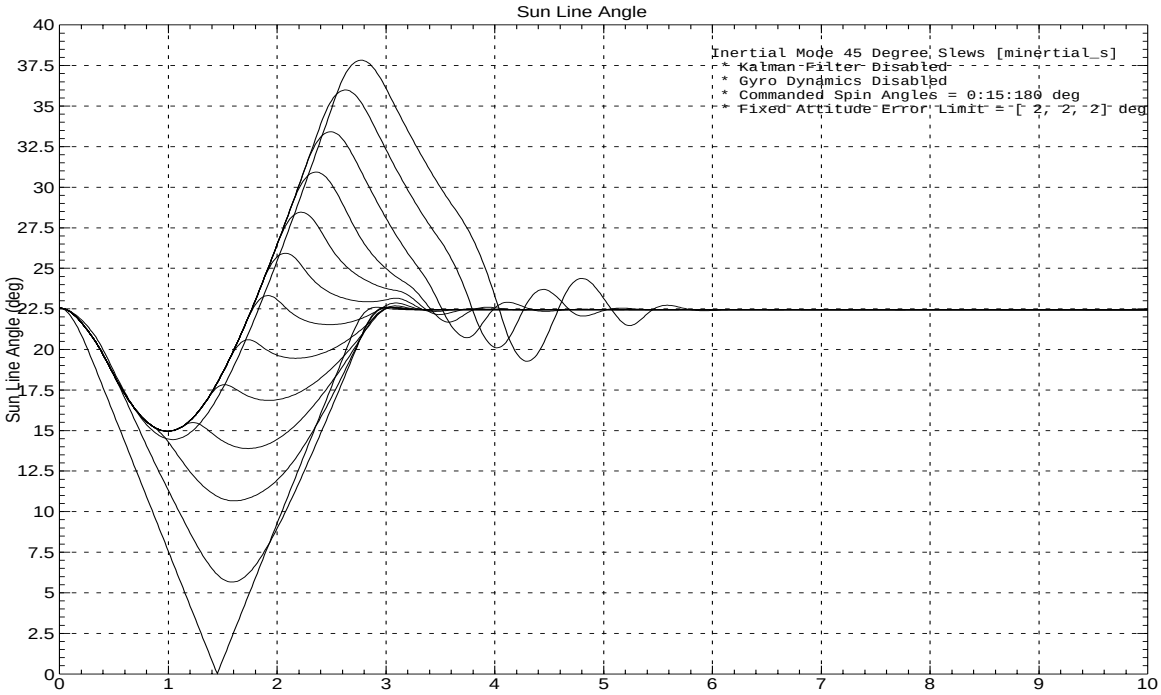

Figure 9. Inertial Mode slews with no dynamic attitude error limiter

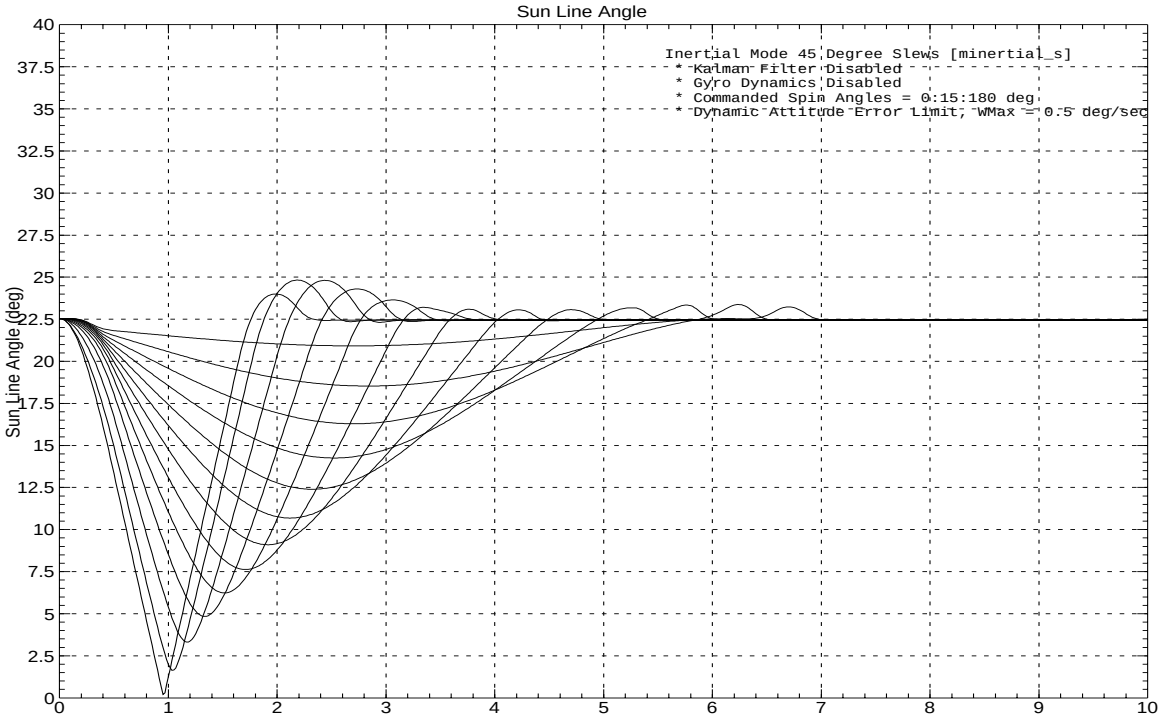

Figure 10. Inertial Mode slews with dynamic attitude error limiter

CONCLUSIONS

The structural system is fairly rigid; therefore, the majority of analysis was done for a plant derived as a combination of the rigid body modes and the chosen dominant flexible modes. Analysis determined that the wheel jitter in resonance with the flexible mode frequencies does not cause problems with MAP's Observing Mode pointing requirements.

All of MAP's operational modes except one satisfied the Guidance Navigation and Control Center design criteria. Since the Safehold Mode Y-axis was unable to meet the required bounds, it was necessary to add a low pass structural filter.

The maximum x and y face aerodynamic torque is 0.012 N-m and the momentum has a peak of 0.47 N-m-s and an average of 0.28 N-m-s. The Earth's gravity gradient an average torque and momentum were calculated to be 2.0×10^{-4} N-m and 0.1744 N-m-s in the x-direction, and 4.1×10^{-5} N-m and 0.221 N-m-s in the z-direction. Gravity gradient simulation results further verified values for torque and momentum buildup. The Earth gravity gradient simulations displayed a maximum torque of 1.7×10^{-4} N-m in the x and y-axes and 1.0×10^{-5} N-m in the z-axis and a maximum momentum of 0.15 N-m-s in the x and y axes, 0.07 N-m-s in the z-axis, and a maximum system momentum of 0.15 N-m-s.

Under ideal conditions, the solar radiation torque about the spin and precession axes average out to zero. However, misalignment of the solar panels can give rise to a pinwheel torque that cause momentum buildup. This situation calls for a maximum allowable solar array deployment misalignment angle is 0.228°. Simulations show that a proposed solution of a three-shot momentum unloading in Observing Mode can be used if the misalignments exceed this limit.

The natural frequency of the slosh system is several orders of magnitude larger than the bandwidth of the system. Therefore, the angular displacement due to either the fuel slosh's linear or angular torque is small and fuel slosh should not be a concern to the MAP mission.

The end result of the analysis is a MAP controller that meets attitude control requirements with margin.

REFERENCES

1. http://map.gsfc.nasa.gov
2. Boggess, N. W., *et al.*, *Astrophysical Journal*, vol. 397, p. 420 (1992).
3. Gulkis, S., Lubin, P. M., Meyer, S. S., and Silverberg, R. F., *Scientific American*, vol. 262, no. 1, p. 132 (1990).
4. Smoot, G. F., *et al.*, *Astrophysical Journal*, vol. 396, p. L1 (1992).
5. The NASTRAN Theoretical Manual", NASA SP-221-(06), COSMIC, University of Georgia, Athens, GA, January 1981.
6. Swales & Associates, Inc., "Modal Significance Analysis Package (MSAP): User's Manual", Technical report SAI-RPT-080, Ver.2, July 1995.
7. Bauer, F.H. and Downing, J., "Control System Design And Analysis Using The INteractive Controls Analysis (INCA) Program", Paper No. 87-2517, AIAA Guidance, Navigation And Control Conference, Monteray, Ca August 1987.

8. Bauer, F.H. and Downing, J., "INteractive Controls Analysis (INCA) Version 2.0", Program Number GSC-12988, COSMIC, University of Georgia, Athens, GA, 1985, updated to Version 3.13, 1989.
9. Wertz, J.R., Spacecraft Attitude Determination and Control, Kluwer Academic Publishers, Dordrecht, Netherlands, 1978.
10. Downing, J., and Surber, J. L., "Solar Pressure and Aerodynamic Drag (SPAD) Version 1.51", NASA in-house software pending publication with COSMIC, 1998.
11. Integrated Systems, Inc., "Matrix$_X$ & SystemBuild User's Guides", January 1996
12. "Study of Liquid Slosh in the Tracking and Data Relay Satellite Hydrazine Tanks", NASA CR 166745, November 1981;
13. Dodge, F.T., "Propellant Dynamics and PMD Design for the Near Earth Asteroid Rendezvous (NEAR) Spacecraft", Southwest Research Institute, SwR Project: 04-6297, Final Report, April 1994.
14. Sirlin, S.W., "Mars Pathfinder Launch Vehicle Nutation Analysis", Jet Propulsion Laboratory, interoffice memo: IOM 3546-96-032, July 19, 1996.
15. Stofan, A., "Experimental Damping of Liquid Oscillations of a Spherical Tank by Positive-Expulsion Bags and Diaphragms", NASA Technical Note D-1311, July 1962.